ENGINEERING TRANSACTIONS • *Engng. Trans.* • **43**, 1–2, 183–204, 1995
Polish Academy of Sciences • Institute of Fundamental Technological Research

A COMPARATIVE STUDY OF VIBRATIONS OF ELASTO-VISCOPLASTIC SHELLS AND PLATES (*)

P. KŁOSOWSKI (GDAŃSK)

K. WOŹNICA and D. WEICHERT (LILLE)

A method of solution of the problem of nonlinear vibrations of elasto-viscoplastic plates and shells is presented, based on the first order shear deformation-moderate rotation theory of the laminated shells. Viscoplastic material behaviour is taken into account by the models developed by Perzyna, Chaboche and Bodner–Partom, respectively. The equations of motion are integrated by the central difference method, while the constitutive equations are integrated by the trapezoidal rule in an iterative process. In both cases the same time step is used. Numerical examples and comparison with experimental results are presented.

1. Introduction

The modelling of vibrations of inelastic structures may lead to incorrect results if visco-plastic effects are ignored. These effects are particularly important when metal alloys under high temperature conditions are considered. Theoretical analyses and experimental studies of the dynamics of inelastic structures have been the subject of a large number of studies. A review of the relevant literature can be found in [1]. Here we recall only those contributions which take into account the phenomenon of viscoplasticity in the response to impulsively loaded plates [2–10] and shells [2, 11–17]. Exact solutions have been obtained only for the simplest cases of symmetric structures (infinite [4] and circular [6] plates or spheres [11, 14, 16]) for small deflections. In [12], the Fourier series have been used to analyse the dynamic behaviour of cylindrical shells. To integrate directly the nonlinear differential equations of motion, the Runge–Kutta method has been applied in [16] for spherical shells. The eigenvalue method is the basis of calculations of rectangular [5] and circular [3, 6] impulsively loaded plates. Various approximation techniques were introduced to solve specific boundary value problems in the

(*) Paper presented at 30th Polish Solid Mechanics Conference, Zakopane, September 5–9, 1994.

range of large deflections. We cite here the methods of finite differences [2, 9], of perturbations [14, 15], and instantaneous modes [7, 8]. Simple analytical expressions for dynamic deflections of thin viscoplastic shells have been given in [13, 17]. A simplified solution of the large deflection problem of thin circular plates can be found in [10].

The majority of this paper concerns the solution based on the linear [3–6, 9–13, 17] or nonlinear [7–10, 14–16] constitutive laws of viscoplasticity by Perzyna. The elasto-viscoplastic material behaviour has been taken into account in two [2, 16] papers only and the hardening effects have been neglected everywhere, with exception of [2]. Results of experimental studies are given, among others, in [2, 3, 6, 18, 19] concerning the response of circular plates and hemispherical shells [2, 13, 17, 20].

In this paper the problem of the nonlinear vibrations of elasto-viscoplastic plates and shells in the context of the first order shear deformation theory at moderate rotations and small strains is studied. The problem is discretized by finite elements. To analyse the dynamic response of structures, three different constitutive laws are used, which are the models developed by Perzyna, Chaboche and Bodner-Partom. The Chaboche and Bodner-Partom's formulations allow to introduce kinematic and isotropic hardening. The proposed method is illustrated by the simulation of the vibration of plates and shells under impulsive loading.

2. Elements of the applied theory of laminated structures

For the present study, the first order shear deformation theory valid for large displacements and restricted to moderate rotations and small strains was chosen. In this chapter, only some basic features of this theory are exposed, details can be found e.g. in [21–23].

In this theory, all field quantities defined in the shell volume $\mathcal{V}$ are referred to the middle surface $\mathcal{M}$ of the shell in its initial (reference) configuration. On this surface, a set of curvilinear coordinates θ^α, $\alpha = 1, 2$ with base vectors $\mathbf{a}_\alpha$ and coordinate θ in direction of the unit normal vector $\mathbf{n}$ of $\mathcal{M}$ is chosen. Then, the displacement vector $\mathbf{V}$ of a characteristic particle of the shell is expressed by

$$\mathbf{V} = \nu_\alpha \mathbf{a}^\alpha + \nu_3 \mathbf{n},$$

where ν_α and ν_3 are the scalar-valued vector components. In the first order shear deformation theory, the displacement field through the shell thickness is approximated by the linear functions

$$\nu_\alpha = \overset{0}{\nu}_\alpha + \theta \overset{1}{\nu}_\alpha, \qquad \nu_3 = \overset{0}{\nu}_3,$$

and the components of the Green strain tensor can be expressed by

$$(2.1)\qquad E_{\alpha\beta} = \overset{0}{E}_{\alpha\beta} + \theta \overset{1}{E}_{\alpha\beta} + \theta^2 \overset{2}{E}_{\alpha\beta}, \quad E_{\alpha 3} = \overset{0}{E}_{\alpha 3} + \theta \overset{1}{E}_{\alpha 3}, \quad E_{33} = \overset{0}{E}_{33},$$

where

$$\begin{aligned}
\overset{0}{E}_{\alpha\beta} &= \overset{0}{\Phi}_{\alpha\beta} + \frac{1}{2} \overset{0}{\varphi}_{3\alpha} \overset{0}{\varphi}_{3\beta},\\
\overset{1}{E}_{\alpha\beta} &= \overset{1}{\Phi}_{\alpha\beta} - \frac{1}{2}\left(b_\alpha^\lambda \overset{0}{\varphi}_{\lambda\beta} + b_\beta^\lambda \overset{0}{\varphi}_{\lambda\alpha}\right) + \frac{1}{2}\left(\overset{0}{\varphi}_{3\alpha} \overset{1}{\varphi}_{3\beta} + \overset{1}{\varphi}_{3\alpha} \overset{0}{\varphi}_{3\beta}\right),\\
\overset{2}{E}_{\alpha\beta} &= -\frac{1}{2}\left(b_\alpha^\lambda \overset{1}{\varphi}_{\lambda\beta} + b_\beta^\lambda \overset{1}{\varphi}_{\lambda\alpha}\right) + \frac{1}{2} \overset{1}{\varphi}_{3\alpha} \overset{1}{\varphi}_{3\beta},\\
\overset{0}{E}_{\alpha 3} &= \frac{1}{2}\left(\overset{0}{\varphi}_{3\alpha} + \overset{1}{\nu}_\alpha\right) + \frac{1}{2} \overset{1}{\nu}{}^\lambda \overset{0}{\varphi}_{3\lambda},\\
\overset{1}{E}_{\alpha 3} &= \frac{1}{2} \overset{1}{\nu}{}^\lambda \overset{1}{\nu}_{\lambda|\alpha}, \qquad \overset{0}{E}_{33} = \frac{1}{2} \overset{1}{\nu}{}^\lambda \overset{1}{\nu}_\lambda
\end{aligned}$$

with

$$\begin{aligned}
\overset{n}{\Phi}_{\alpha\beta} &= \frac{1}{2}\left(\overset{n}{\nu}_{\alpha|\beta} + \overset{n}{\nu}_{\beta|\alpha}\right) - b_{\alpha\beta} \overset{n}{\nu}_3,\\
\overset{n}{\varphi}_{\alpha\beta} &= \overset{n}{\nu}_{\alpha|\beta} - b_{\alpha\beta} \overset{n}{\nu}_3,\\
\overset{n}{\varphi}_{3\alpha} &= \overset{n}{\nu}_{3,\alpha} + b_\alpha^\lambda \overset{n}{\nu}_\lambda .
\end{aligned}$$

Here, $(\cdot)_{,\alpha}$ and $(\cdot)_{|\alpha}$ stand for partial and covariant differentiation on $\mathcal{M}$, respectively, and $b_{\alpha\beta}$, b_α^λ denote the covariant and mixed components of the curvature tensor on $\mathcal{M}$.

As usual, to transform the differential element of volume $d\mathcal{V}$ and the surface element $d\mathcal{A}$ to values on the middle surface, the shifter tensor $\mathbf{c}$ is introduced with

$$c_\alpha^\beta = \delta_\alpha^\beta - \theta b_\alpha^\beta, \qquad d\mathcal{V} = c\,d\theta\,d\mathcal{M}, \qquad d\mathcal{A} = c\,d\mathcal{M}, \qquad c = \det(c_\alpha^\beta).$$

The field equations for the shell problem are derived with the help of the principle of virtual work, given in its general form by

$$(2.2)\qquad \int_{\mathcal{V}} \left\{ s^{ij}\,\delta E_{ij}(\mathbf{V}) - \rho(F^i - I^i)\delta V_i \right\} d\mathcal{V} - \int_{\mathcal{A}} {}^*s^i\,\delta V_i\,d\mathcal{A} = 0,$$

where s^{ij} are the components of the second Piola–Kirchhoff stress tensor, ρ denotes the material density in the undeformed configuration, F^i, I^i, ${}^*s^i$ are the components of body forces, inertia forces and external surface forces, respectively.

If, in contrast to methods of global estimations of the behaviour of inelastic structures, e.g. in limit analysis or shakedown analysis, the evolution as a function of time has to be simulated, it seems to be more appropriate to use layered models that allow to follow the evolution of the material properties in each layer separately. For this the volume of the structure is divided into L layers parallel to $\mathcal{M}$. Then, the principle of virtual work (2.2) reduces to the well known form for laminated shells theory

$$\int_{\mathcal{M}} \sum_{k=0}^{L} \left\{ \sum_{n=0}^{2} {}^{n}_{k}L^{\alpha\beta}\, \delta {}^{n}_{}E_{\alpha\beta} + 2 \sum_{n=0}^{1} {}^{n}_{k}L^{\alpha 3}\, \delta {}^{n}_{}E_{\alpha 3} + {}^{0}_{k}L^{33}\, \delta {}^{0}_{}E_{33} \right.$$

$$\left. - \sum_{n=0}^{1} \left[\left({}^{n}_{k}F^{\alpha} - {}^{n}_{k}I^{\alpha} + {}^{n}_{}p^{\alpha} \right) \delta {}^{n}_{}\nu_{\alpha} \right] + \left({}^{0}_{k}F^{3} - {}^{0}_{k}I^{3} + {}^{0}_{}p^{3} \right) \delta {}^{0}_{}\nu_{3} \right\} d\mathcal{M}$$

$$- \int_{\mathcal{L}} \sum_{k=1}^{L} \left[\sum_{n=0}^{1} \left({}^{*}{}^{n}_{k}L^{\alpha}\, \delta {}^{n}_{}\nu_{\alpha} + {}^{*}{}^{0}_{k}L^{3}\, \delta {}^{0}_{}\nu_{3} \right) \right] d\mathcal{L} = 0 \tag{2.3}$$

with

$${}^{n}_{k}L^{ij} = \int_{z_k}^{z_{k+1}} {}^{k}c^{k}s^{ij}\theta^{n}\, d\theta,$$

$${}^{n}_{}I^{i}_{k} = \sum_{q=1}^{1} {}^{q+n}_{i\,k}\ddot{\nu}^{q_i}, \qquad {}^{r}_{ik} = \int_{z_k}^{z_{k+1}} {}^{k}\rho\, {}^{k}c\theta^{r}\, d\theta, \tag{2.4}$$

$${}^{n}_{k}F^{i} = \int_{z_k}^{z_{k+1}} {}^{k}\rho\, {}^{k}c\, {}^{k}f^{i}\theta^{n}\, d\theta,$$

where ${}^{k}f^{i}$ $(i = 1, 2, 3)$ are the body force components of layer k measured per unit volume of the undeformed body. z_k, z_{k+1} are the coordinates of lower and upper surface of the k-th layer in θ-direction, ${}^{n}_{}p^{i} = [c\overline{p}^{i}\theta^{n}]\Big|_{z_1}^{z_L}$ are the components of the surface loads, and ${}^{*}{}^{n}_{k}L^{i}$ are the components of the stress tensor defined on the boundary curve $\mathcal{L}$ of the middle surface $\mathcal{M}$, calculated in a similar way as the couples ${}^{n}_{k}L^{ij}$.

After discretization by finite elements (details of this transformation can be found in [1]), we obtain a system of nonlinear equations of motion

$$\mathbf{M}\,\ddot{\mathbf{q}} + \mathbf{Q} = \mathbf{R}, \tag{2.5}$$

where $\mathbf{M}$ is the mass matrix, $\mathbf{Q}$ are the balanced forces in the actual configuration containing all nonlinear effects and $\mathbf{R}$, $\ddot{\mathbf{q}}$ are the external loads and the nodal accelerations, respectively.

3. Constitutive relations

3.1. General assumptions

It is assumed, that strains are small enough so that the additive decomposition of their rates $\dot{\mathbf{E}}$ into a purely elastic part $\dot{\mathbf{E}}^E$ and an inelastic part $\dot{\mathbf{E}}^I$ is justified:

$$\dot{\mathbf{E}} = \dot{\mathbf{E}}^E + \dot{\mathbf{E}}^I.$$

Then, the rates of the second Piola–Kirchhoff stress tensor can be expresed by

$$\dot{\mathbf{s}} = \mathbf{D} : \dot{\mathbf{E}}^E = \mathbf{D} : (\dot{\mathbf{E}} - \dot{\mathbf{E}}^I), \tag{3.1}$$

where $\mathbf{D}$ is the generalised tensor of elastic coefficients, assumed to be constant.

In the case of layered models, the representatives of stresses and distributed forces referred to the midsurface $\mathcal{M}$ of the shell are obtained by integration over the shell thickness. Let $\mathbf{Q}^T$ be the vector of these representatives, defined by

$$\mathbf{Q}^T = \left\{ \overline{\mathbf{N}} \quad \overline{\mathbf{M}} \quad \overline{\mathbf{P}} \quad \overline{\mathbf{Q}}_1 \quad \overline{\mathbf{Q}}_2 \right\},$$

where the components of this generalised vector are given by

$$\begin{aligned} \overline{\mathbf{N}}^T &= \left\{ \overset{0}{R}{}^{11} \quad \overset{0}{R}{}^{22} \quad \overset{0}{R}{}^{12} \right\}, \\ \overline{\mathbf{M}}^T &= \left\{ \overset{1}{R}{}^{11} \quad \overset{1}{R}{}^{22} \quad \overset{1}{R}{}^{12} \right\}, \\ \overline{\mathbf{P}}^T &= \left\{ \overset{2}{R}{}^{11} \quad \overset{2}{R}{}^{22} \quad \overset{2}{R}{}^{12} \right\}, \end{aligned} \tag{3.2}$$

$$\overline{\mathbf{Q}}_1^T = \left\{ \overset{0}{R}{}^{23} \quad \overset{0}{R}{}^{13} \right\}, \qquad \overline{\mathbf{Q}}_1^T = \left\{ \overset{1}{R}{}^{23} \quad \overset{1}{R}{}^{13} \right\} \tag{3.3}$$

with

$$\overset{n}{R}{}^{\alpha j} = \sum_{k=1}^{L} \overset{n}{R}{}_k^{\alpha j} = \sum_{k=1}^{L} \int_{z_k}^{z_{k+1}} cs^{\alpha j} \theta^n \, d\theta = \sum_{k=1}^{L} \frac{1}{n+1} cs^{\alpha j} \left[(z_{k+1})^{n+1} - (z_k)^{n+1} \right].$$

Thus, the local evolution of the material properties can be layerwise approximated without loosing the advantage a two-dimensional formulation of the problem by means of the shell theory.

3.2. Elasto-vicoplastic constitutive equations

To evaluate the stress rates using formula (3.1), the inelastic strain rates $\dot{\mathbf{E}}^I$ must be determined. A large class of constitutive models can be represented by the following mathematical form

$$\dot{\mathbf{E}}^I = f(\mathbf{s}, \mathbf{X}, T),$$
$$\dot{\mathbf{X}} = g(\dot{\mathbf{E}}^I, \mathbf{X}, T),$$

where the inelastic strain rates $\dot{\mathbf{E}}^I$ are defined as a function of the stress $\mathbf{s}$, temperature T, and a set of internal variables $\mathbf{X}$. In this paper, three different constitutive models are applied, which are the models of PERZYNA [24], CHABOCHE [25] and BODNER–PARTOM [26]. A detailed discussion of these models can be found in [27]. Here, the most important relations characterising these models are given in Table 1. It should be noted that, in contrast to the formulations by Perzyna and Chaboche, the Bodner - Partom constitutive law does not introduce the notion of yield surface. As it can be easily observed, the models of Chaboche and of Perzyna coincide if we assume $K = k$ and if hardening is neglected. It is important to note that the Perzyna and Bodner - Partom models can be used for a large range of strain rates. On the other hand, the Chaboche model was formulated only for low strain rates, what is confirmed by the comparison of the numerical results.

4. THE FINITE ELEMENT FORMULATION

4.1. Element description

The finite element method was chosen for the discretization of the problem and to prepare its numerical solution. The nine-node isoparametric finite elements shown in Fig. 1 were used to discretise the whole structure. Tensorial and vectorial quantities of Eqs. (2.4) and (2.5) are integrated over the thickness of the finite element using the Gauss scheme. By the usual aggregation process the system of equations for the entire discretized structure is obtained. The present matrix form is valid for plates, cylindrical and spherical shells.

4.2. Integration of constitutive equations

The elasto-viscoplastic model of constitutive equations has a differential form. Generally, a numerical method for their integration has to be used.

Table 1.

	Perzyna model	Chaboche model	Bodner – Partom model
Inelastic strain rate	$\dot{\mathbf{E}}^I = \frac{3}{2}\,\dot{p}\,\frac{\mathbf{s}'}{J(\mathbf{s}')}$	$\dot{\mathbf{E}}^I = \frac{3}{2}\,\dot{p}\,\frac{\mathbf{s}'-\mathbf{X}'}{J(\mathbf{s}'-\mathbf{X}')}$	$\dot{\mathbf{E}}^I = \frac{3}{2}\,\dot{p}\,\frac{\mathbf{s}'}{J(\mathbf{s}')}$
Deviatoric part of tensor	$\mathbf{s}' = \mathrm{dev}\,(\mathbf{s}) = \mathbf{s} - \frac{1}{3}\,\mathrm{tr}\,(\mathbf{s})\mathbf{I}$		
Cumulative equivalent of inelastic strain	$\dot{p} = \gamma \left\langle \frac{J(\mathbf{s}')-k}{k} \right\rangle^n$	$\dot{p} = \gamma \left\langle \frac{J(\mathbf{s}'-\mathbf{X}')-R-k}{K} \right\rangle^n$	$\dot{p} = \frac{2}{\sqrt{3}} D_0 \exp\left[-\frac{1}{2}\left(\frac{R+DP}{J(\mathbf{s}')}\right)^{2n}\frac{n+1}{n}\right]$
Additional definitions	$J(\mathbf{a}) = \left(\frac{3}{2}\mathbf{a}:\mathbf{a}\right)^{1/2} = \left(\frac{3}{2}a^{ij}a_{ij}\right)^{1/2}$ $\langle x\rangle = \frac{1}{2}\,(x+\lvert x\rvert)$		$DP = \mathbf{X}:\frac{\mathbf{s}}{J(\mathbf{s})}$ $\dot{W}^I = \mathbf{s}:\dot{\mathbf{E}}^I$
Isotropic hardening function	–	$\dot{R} = b(R_1 - R)\,\dot{p}$	$\dot{R} = m_1(R_1 - R)\,\dot{W}^I - A_1 R_1 \left(\frac{R+R_2}{R_1}\right)^{n_1}$
Kinematic hardening tensor	–	$\dot{\mathbf{X}} = \frac{2}{3}a\,\dot{\mathbf{E}}^I - c\mathbf{X}\,\dot{p}$ $\mathbf{X}' = \mathrm{dev}\,(\mathbf{X}) = \mathbf{X} - 1/3\,\mathrm{tr}\,(\mathbf{X})\mathbf{I}$	$\dot{\mathbf{X}} = m_2\left(\frac{3}{2}D_1\frac{\mathbf{s}}{J(\mathbf{s})} - \mathbf{X}\right)\dot{W}^I - A_2 R_1 \frac{3}{2}\left[\frac{2/3\;J(\mathbf{X})}{R_1}\right]^{n_2}\frac{\mathbf{X}}{J(\mathbf{X})}$
Constitutive equation's constants	γ, k, n	$k, K, n, a, c, b, R_1, \gamma$	$n, n_1, n_2, D_0, D_1, R_0, R_1, R_2, A_1, A_2, m_1, m_2$

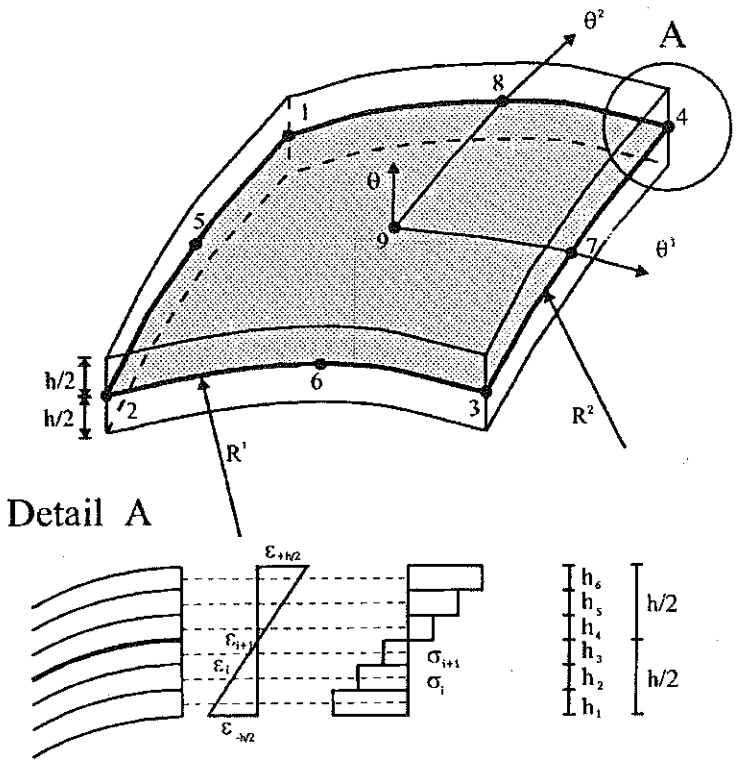

FIG. 1. Finite element and idea of stress approximation.

Here, an explicit procedure of the trapezoidal rule is chosen in order to build an iterative algorithm of integration. This algorithm may be expressed by the following equations

$$\Delta \mathbf{E}^I = \frac{\Delta t}{2}\left[f(\mathbf{s}_{t-\Delta t}, \mathbf{X}_{t-\Delta t}, R_{t-\Delta t}) + f(\mathbf{s}_t, \mathbf{X}_t, R_t)\right] = \frac{\Delta t}{2}\left[\dot{\mathbf{E}}^I_{t-\Delta t} + \dot{\mathbf{E}}^{Ii-1}_t\right],$$

$$\Delta \mathbf{X} = \frac{\Delta t}{2}\left[g(\mathbf{s}_{t-\Delta t}, \mathbf{X}_{t-\Delta t}, R_{t-\Delta t}) + g(\mathbf{s}_t, \mathbf{X}_t, R_t)\right] = \frac{\Delta t}{2}\left[\dot{\mathbf{X}}_{t-\Delta t} + \dot{\mathbf{X}}^{i-1}_t\right],$$

$$\Delta R = \frac{\Delta t}{2}\left[h(\mathbf{s}_{t-\Delta t}, \mathbf{X}_{t-\Delta t}, R_{t-\Delta t}) + h(\mathbf{s}_t, \mathbf{X}_t, R_t)\right] = \frac{\Delta t}{2}\left[\dot{R}_{t-\Delta t} + \dot{R}^{i-1}_t\right],$$

$$\mathbf{E}^I_t = \mathbf{E}^{Ii}_t = \mathbf{E}^I_{t-\Delta t} + \Delta \mathbf{E}^I,$$
$$\mathbf{X}_t = \mathbf{X}^i_t = \mathbf{X}_{t-\Delta t} + \Delta \mathbf{X},$$
$$R_t = R^i_t = R_{t-\Delta t} + \Delta R.$$

Here the index i denotes the number of iteration. The iteration process is carried out until for the each component of inelastic strain $\dot{\mathbf{E}}^I$, the error is

less than the assumed error range η,

$$\left| \frac{\dot{E}_t^{Ii} - \dot{E}_t^{Ii-1}}{\dot{E}_t^{Ii}} \right| < \eta.$$

4.3. Integration of equations of motion

To integrate the nonlinear equations of motion (2.5), the central differences method is applied. This method links the displacement vectors of three succeeding instants of time $\mathbf{q}_{t-\Delta t}$, $\mathbf{q}_t$, $\mathbf{q}_{t+\Delta t}$ with the velocity and the acceleration vectors at time t

$$\begin{aligned} \ddot{\mathbf{q}}_t &= \frac{1}{\Delta t^2}(\mathbf{q}_{t-\Delta t} - 2\mathbf{q}_t + \mathbf{q}_{t+\Delta t}), \\ \dot{\mathbf{q}}_t &= \frac{1}{2\Delta t}(-\mathbf{q}_{t-\Delta t} + \mathbf{q}_{t+\Delta t}), \end{aligned} \tag{4.1}$$

where one and two superposed dots denote, respectively, the first and second derivative with respect of time of the considered quantity. Then at time t the equations of motion according to Eq. (2.5), together with Eqs. (4.1), define the displacement vector at time $t + \Delta t$

$$\mathbf{q}_{t+\Delta t} = \left(\frac{1}{\Delta t^2}\mathbf{M}\right)^{-1} \left[\mathbf{R}_t - \mathbf{Q}_t - \frac{1}{\Delta t^2}\mathbf{M}(\mathbf{q}_{t-\Delta t} - 2\mathbf{q}_t)\right].$$

Just like all explicit methods of integration for the equations of motion, this method needs a starting procedure:

$$\mathbf{q}_1 = \mathbf{q}_0\, \dot{\mathbf{q}}_0\, \Delta t + \frac{1}{2}\, \ddot{\mathbf{q}}_0\, \Delta t^2.$$

The main advantage of the central difference method is that the time-consuming calculation of the stiffness matrix can be avoided. All nonlinear effects are included in the vector of balanced forces $\mathbf{Q}$. This is very helpful in complicated algorithms such as the presented one. The major drawback of this method, however, is the necessity to use a small time step Δt because of the stability limits of the numerical scheme. In the linear case, the critical time step Δt_{cr} can be calculated from the highest natural frequency of the discrete structure $\omega_{\max}$

$$\Delta t_{\mathrm{cr}} = 2/\omega_{\max}.$$

It turned out that also in the nonlinear calculations presented in this paper this condition is strong enough to assure the stability of integration. Additionally it was noticed that in most cases the time step calculated by this method is also small enough to assure the stability of the integration of the constitutive equations by the trapezoidal rule.

5. Examples

The method developed is applied to the simulation of the dynamic response of rectangular plates and cylindrical shells under impulsive loads. Here, the results obtained by means of the three aforementioned constitutive models are presented.

5.1. *Rectangular plate under suddenly applied uniformly distributed loading*

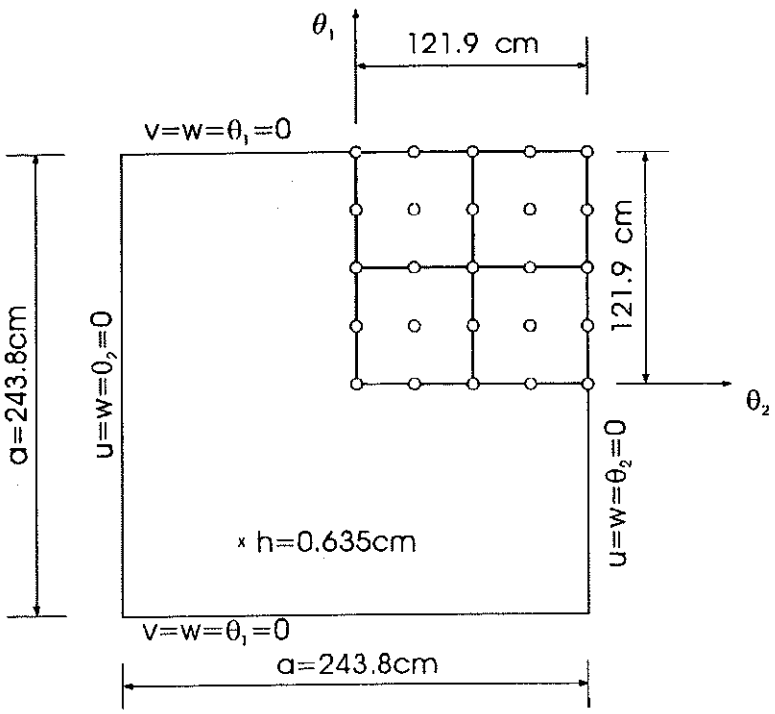

FIG. 2. The geometry and finite element mesh of the simply supported plate.

The behaviour of an INCO 718 alloy plate (Fig. 2) was simulated using the Chaboche and Bodner - Partom model. The following values of material properties were used:

Chaboche model at $T = 800°$ C [27]:

$$E = 140.3\,\text{GPA}, \quad \gamma = 1\,\text{s}^{-1}, \quad n = 4, \quad k = 211.0\,\text{MPa},$$
$$K = 2171.0\,\text{MPa}, \quad c = 500.0, \quad a = 170.0\,\text{GPa}, \quad R_1 = -203.7\,\text{MPa},$$
$$b = 60.0, \quad \nu = 0.3, \quad \rho = 7.9 \cdot 10^3\,\text{MNs/m}^4,$$
$$\Delta t_{\text{cr}} = 1.5024 \cdot 10^{-6}\,\text{s}, \quad \Delta t = 1.50 \cdot 10^{-6}\,\text{s};$$

Chaboche model at $T = 650°$ C [28]:

$$E = 159.0\,\text{GPa}, \quad \gamma = 1\,\text{s}^{-1}, \quad n = 4, \quad k = 514.21\,\text{MPa},$$
$$K = 1025.51\,\text{MPa}, \quad c = 500.0, \quad a = 170.0\,\text{GPa}, \quad R_1 = -194.39\,\text{MPa},$$
$$b = 60.0, \quad \nu = 0.3, \quad \rho = 7.9 \cdot 10^3\,\text{MNs}^2/\text{m}^4,$$
$$\Delta t_{\text{cr}} = 1.44 \cdot 10^{-6}\text{s}, \quad \Delta t = 11.40 \cdot 10^{-6}\,\text{s};$$

Bodner–Partom model at $T = 650°$ C [29]:

$$E = 169.0\,\text{GPa}, \quad n = 1.17, \quad R_0 = 3130.0\,\text{MPa},$$
$$R_1 = 4140.0\,\text{MPa}, \quad R_2 = 2760.0\,\text{MPa}, \quad m_1 = 0.024\,\text{MPa}^{-1},$$
$$A_1 = A_2 = m_2 = D_1 = 0, \quad D_0 = 10^4\,\text{s}^{-1}, \quad n_1 = 2.86,$$
$$\nu = 0.3, \quad \rho = 7.9 \cdot 10^3\,\text{MNs}^2/\text{m}^4,$$
$$\Delta t_{\text{cr}} = 1.399 \cdot 10^{-6}\,\text{s}, \quad \Delta t = 1.35 \cdot 10^{-6}\text{s}.$$

First, the accuracy of the distribution of stresses through the thickness of the plate was checked. To cause vibrations of the plate in the elastic range only, a suddenly applied load $q = 0.0001$ MPa was chosen and the calculation was performed for the Chaboche model at $T = 800°$ C. The comparison with the results for displacements, velocities and accelerations obtained for the purely elastic model, where the exact integration of stresses over the plates thickness is performed, shows (Fig. 3) that at least four layers are necessary to get a good correlation between the exact and the approximate calculation method.

The same plate at the same temperature was then suddenly subjected to the uniformly distributed load $q = 1.0$ MPa causing elasto-viscoplastic vibrations. An eight-layer model was applied. The difference between the purely elastic vibration and elasto-viscoplastic vibrations obtained using the Chaboche model is expressed in Fig. 4 for a short time vibration. One observes that the values of the lowest limit for the displacement grows, a phenomenon that becomes even more visible for the longer time simulations, shown in Fig. 5.

In Fig. 6 the same plate is examined at temperature 650° C. In this case, the amplitude of vibrations obtained using the Chaboche model (Fig. 6a) is quite different from vibrations at 800° C. The values of the maximum displacement did not change but the amplitudes of vibrations are smaller at 650° C. The Bodner–Partom model solution compared with the Chaboche solution (Fig. 6b) gives larger values of the displacements at smaller amplitudes. This may be explained by the difference of the ranges of the strain rates for which the constitutive parameters were determined. The elastic solutions (Fig. 6c) of course coincide.

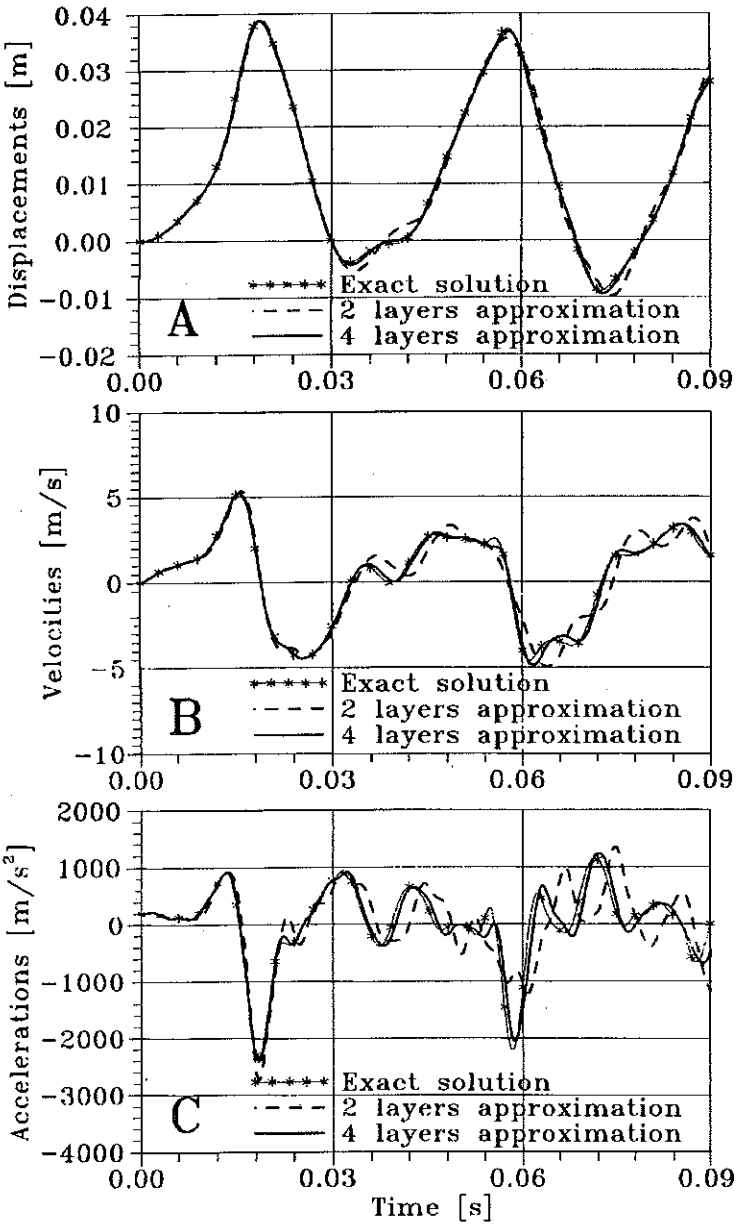

FIG. 3. INCO 718 ($T = 800°$ C) plate, middle point vibrations, $q = 0.0001$ MPa; a) displacements, b) velocities, c) accelerations.

In plates subjected to the load $q = 1.0$ MPa, on the hinged edges of the plate, the rotations exceed, for the extreme positions of the plate, the condition of moderate rotations. However, this local effect appearing for

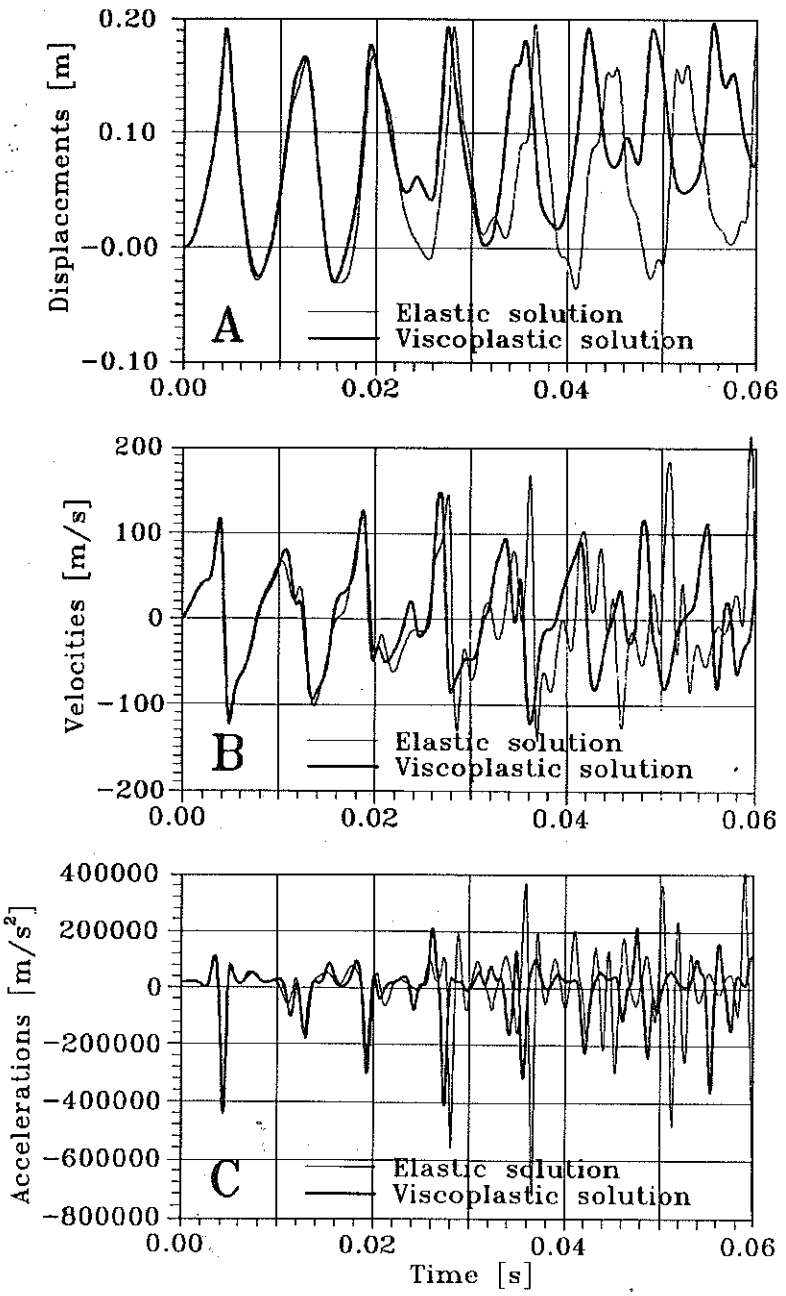

FIG. 4. INCO 718 ($T = 800°$ C) plate, middle point vibrations, $q = 1.0$ MPa; a) displacements, b) velocities, c) accelerations (short time).

very short times has, in the authors' opinion, no great influence on the total solution.

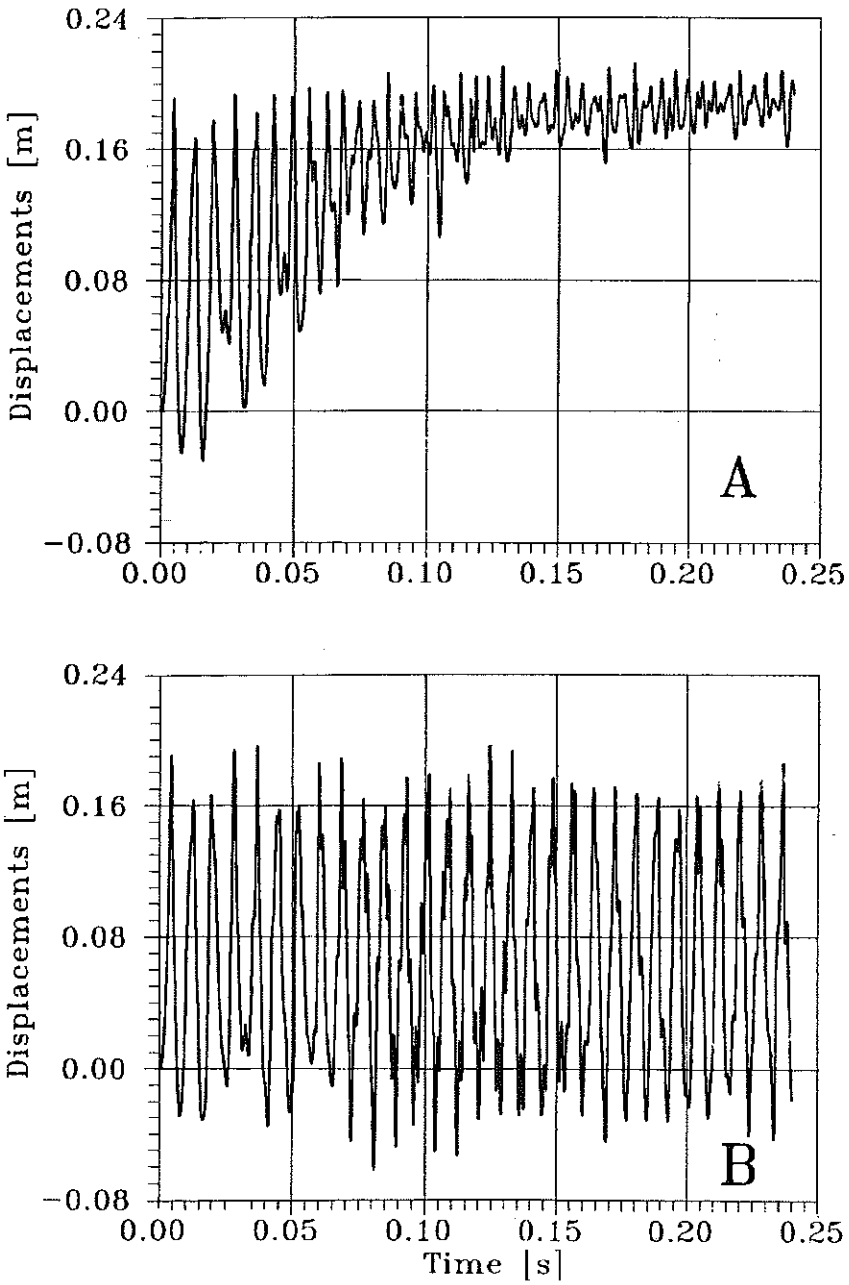

FIG. 5. Long time vibration of INCO 718 ($T = 800°$ C) plate, middle point vibrations, $q = 1.0$ MPa, a) Chaboche model, b) elastic solution.

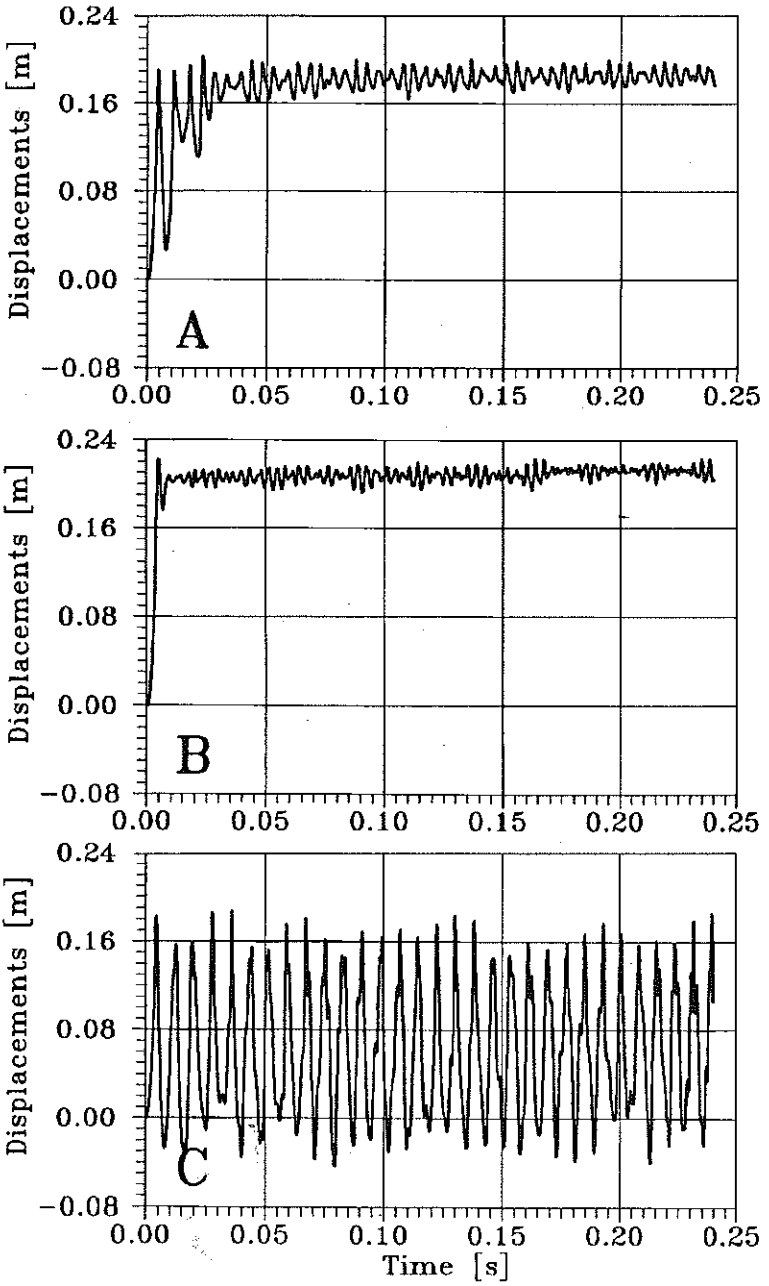

FIG. 6. Long time vibration of INCO 718 ($T = 650°$ C) plate, middle point vibrations, $q = 1.0$ MPa, a) Chaboche model, b) Bodner–Partom model, c) elastic solution.

5.2. *Cylindrical shell under distributed loading*

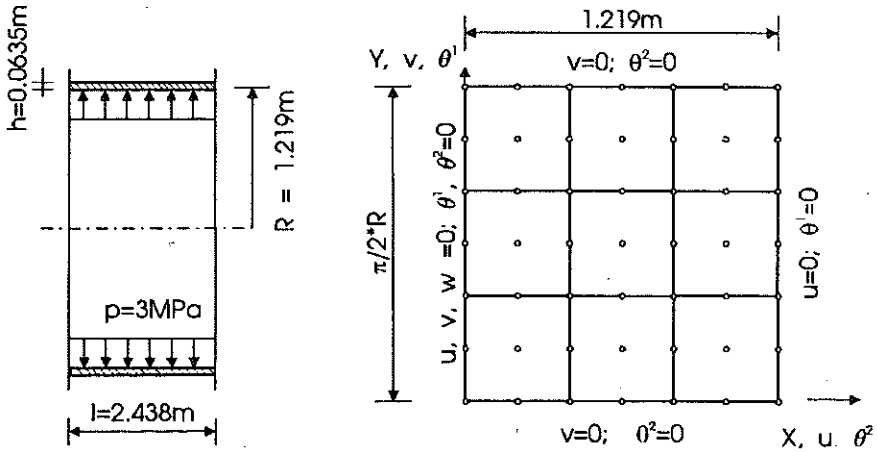

FIG. 7. The geometry and finite element mesh of clamped cylindrical shell.

A cylindrical four-layers shell (Fig. 7) was subjected to a suddenly applied uniformly distributed loading $p = 3$ MPa. This example was examined using all three constitutive models. Material coefficients of the INCO 718 at 650° C were the same as in the plate example. For the Bodner – Partom and Perzyna models the material parameters were adjusted so that the same yield stress at the same initial strain rate as in the Chaboche model is obtained:

Bodner-Partom model:

$$E = 159.0\,\text{GPa}, \quad n = 1.17, \quad R_0 = 3130.0\,\text{MPa}, \quad R_1 = 4140.0\,\text{MPa},$$
$$m_1 = 0.024\,\text{MPa}^{-1}, \quad A_1 = A_2 = m_2 = D_1 = 0, \quad D_0 = 54\,\text{s}^{-1},$$
$$\nu = 0.3, \quad \rho = 7.9 \cdot 10^3\,\text{MNs}^2/\text{m}^4, \quad \Delta t = 1.4 \cdot 10^{-6}\text{s};$$

Perzyna model:

$$k = 514.21\,\text{Mpa}, \quad n = 4, \quad \gamma = 0.0632\,\text{s}^{-1}.$$

This choice leads to a good agreement between the results for the three models, especially displacement in the beginning of the process (Fig. 8). For longer times, differences appear due to the different modelling of hardening in each constitutive model. Perzyna neglects hardening, Bodner – Partom consider isotropic hardening only and Chaboche takes isotropic hardening (softening in the case of the INCO 718 at 650° C) and kinematic hardening into account.

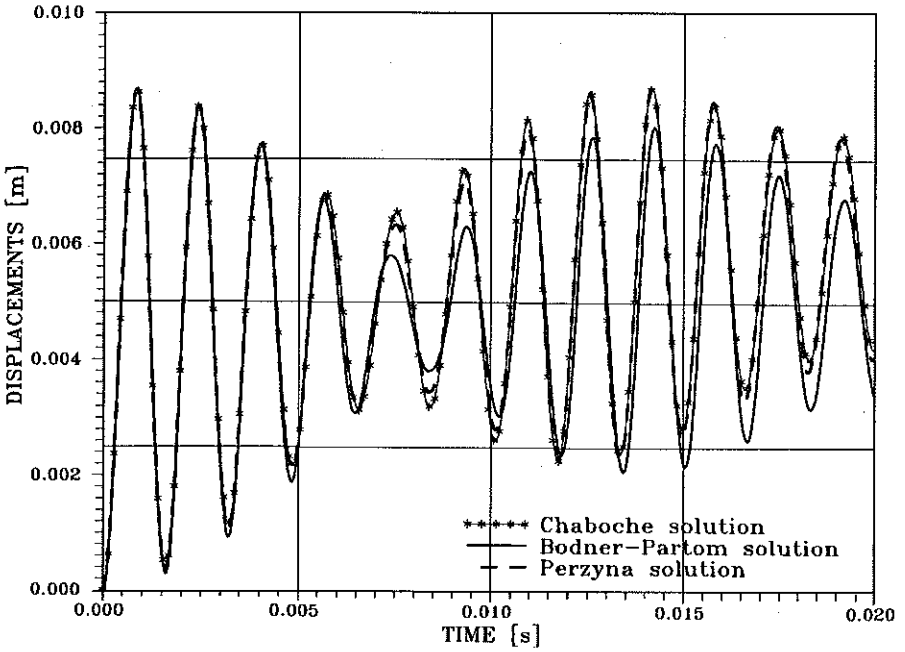

FIG. 8. Middle point vibrations.

5.3. Cylindrical panel under explosive loading

A cylindrical panel [19, 30–32] as shown in Fig. 9, made of a 6061-T6 aluminium alloy is subjected to an explosive type of loading on the indicated area. The explosion is simulated by initial velocities $v_0 = 143.51$ m/s of the shell surface normal to M. One half of the symmetric structure was divided into 4×16 nine-node finite elements and into four layers. In Fig. 10 the

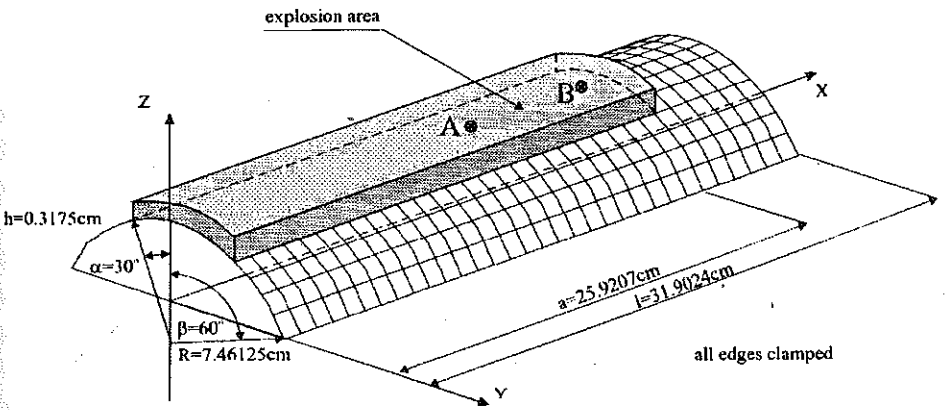

FIG. 9. The geometry of cylindrical panel with all edges clamped under explosive loading.

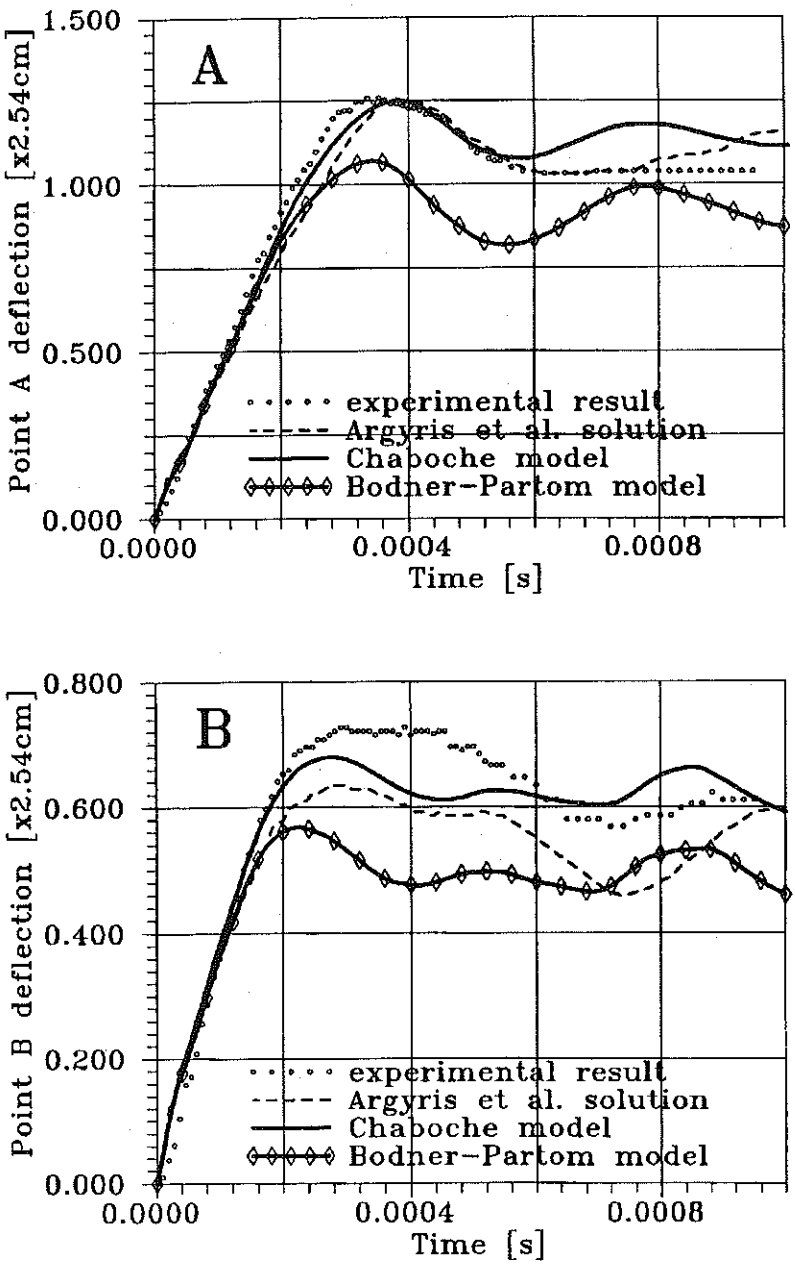

FIG. 10. a) Vibrations of point A ($X = 15.9512\,\text{cm}$), b) vibrations of point B ($X = 23.9268\,\text{cm}$).

vibrations of points A and B are compared with the experimental data from [19] and with the results of perfect plastic calculations from [30]. The

presented Chaboche model calculations were performed with the following physical parameters

$$E = 73.0\,\text{MPa}, \quad \gamma = 1.0\,\text{s}^{-1}, \quad n = 1, \quad k = 303.48\,\text{MPa}, \quad K = 1.0\,\text{MPa},$$

$$a = b = c = R_1 = 0, \quad \nu = 0.3, \quad \rho = 2.67\,\text{MNs}^2/\text{m}^4,$$

$$\Delta t_{\text{cr}} = 5.84 \cdot 10^{-7}\,\text{s}, \quad \Delta t = 10^{-8}\,\text{s}.$$

The parameters for the Bodner–Partom model were taken from [33]

$$E = 73.9\,\text{GPa}, \qquad n = 5.0, \qquad R_0 = 450\,\text{MPa}, \qquad R_1 = 550\,\text{MPa},$$

$$m = 0.12\,\text{MPa}^{-1}, \quad A_1 = A_2 = m_2 = D_1 = R_2 = n_1 = 0, \quad D_0 = 10^8\,\text{s}^{-1},$$

$$\nu = 0.3, \qquad \rho = 2.67 \cdot 10^{-3}\,\text{MNs}^2/\text{m}^4, \qquad \Delta t = 10^{-8}\,\text{s}.$$

It was found that the Chaboche model gives a solution which is in a very good agreement with both the experimental and [19] numerical results. Two configurations of the shell in a deformed state are presented in Fig. 11.

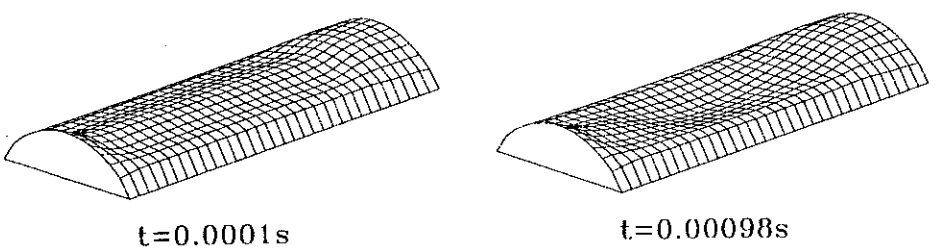

FIG. 11. Configurations of deformed panel.

6. CONCLUSIONS

The proposed method of simulation of the dynamic behaviour of elasto-viscoplastic plates and shells was verified and illustrated by several examples. Three constitutive models have been examined. The major difficulty for the validation of the model was to find sets of material data for the same material available for different models of the constitutive equations. In the material data accessible in the literature even for the same material, at the same temperature and for the same constitutive law, significant differences of the parameters can be found. A major problem in the validation procedure of the simulation procedure of the program is the lack of a broader data base for material parameters, and of a sufficient number of experimental results. However, the authors are aware of the difficulties encountered in this type of

experimental investigations. The examples presented in Figs. 6 and 10 show that the results of numerical investigations of vibrations are very sensitive to the variation of material parameters.

For the cylindrical shell (Fig. 8), a good agreement of results obtained with the different constitutive models was observed. In the Chaboche model, both kinds of the hardening were introduced; because of lack of data, in the Bodner-Partom model only isotropic hardening was taken into account. In the Perzyna model both kinds of the hardening were not considered.

Nonlinear dynamic calculations, even in the purely elastic case, are very time-consuming. This situation gets worse if additionally the constitutive equations have to be integrated due to their incremental nature. The calculations of the balanced forces through layers and especially the iteration process need a large size of the computer memory, necessary to store the information on the material history of two last time steps.

The central differences method used for the integration of the equations of motion requires small time steps. Generally, their values are small enough to integrate also the constitutive equations. In very rapid processes only, like explosions, smaller time steps for the integration of the constitutive equations are required. More sophisticated methods of integration of the equations of motion would allow for bigger time steps, but then it could happen that different time steps for the integration of the equations of motion and the constitutive relations would be needed.

In the proposed algorithm, the calculations of the stiffness matrix are not required. The multiplications of rather small matrices are needed only on the level of single elements. Also it is not necessary to solve the full system of equations, as it is usually the case in explicit methods.

The inclusion of the viscoplastic effects into dynamics calculations causes a fast decrease of the amplitude of vibrations which is a kind of damping effect. The difference to elastic damping is that both the upper and lower amplitudes decrease; in viscoplasticity, to the contrary, only the lower amplitude decreases.

REFERENCES

1. P. KŁOSOWSKI, K. WOŹNICA and D. WEICHERT, *Dynamics of elasto-viscoplastic plates and shells*, Arch. Appl. Mech., 1995 [in print].

2. E.A. WITMER, H.A. BALMER, J.W. LEECH and T.H.H. PIAN, *Large dynamic deformations of beams, rings, plates and shells*, AIAA J., 1, 8, 1848–1858, 1963.

3. T. WIERZBICKI, *Impulsive loading of rigid viscoplastic plates*, Int. J. Solids Struct., **3**, 635–647, 1967.

4. C.A. CALDER, J.M. KELLY and W. GOLDSMITH, *Projectile impact on an infinite viscoplastic plate*, Int. J. Solids Struct., **7**, 1143–1152, 1971.

5. W. WOJEWÓDZKI and T. WIERZBICKI, *Transient response of viscoplastic rectangular plates*, Arch. Mech., **24**, 4, 587–604, 1972.

6. T. WIERZBICKI and A.L. FLORENCE, *A theoretical and experimental investigation of impulsively loaded clamped circular viscoplastic plates*, Int. J. Solids Struct., **13**, 865–876, 1977.

7. CH.T. CHON and P.S. SYMONDS, *Large dynamic plastic deflection of plates by mode method*, J. Engng. Mech. Division, Proc. ASCE, **103**, DEM1, 3–14, 1977.

8. P.S. SYMONDS and CH.T. CHON, *Finite viscoplastic deflections of an impulsively loaded plate by the mode approximation technique*, J. Appl. Math. Phys. Solids, **27**, 115–133, 1979.

9. W. IDCZAK, CZ. RYMARZ and A. SPYCHAŁA, *Large deflection of a rigid-viscoplastic impulsively loaded circular plate*, J. Tech. Phys., **21**, 4, 473–487, 1980.

10. W. IDCZAK, *Approximate solutions in dynamics of inelastic membranes. Part I* [in Polish], Engng. Trans., **33**, 4, 519–535, 1985.

11. T. WIERZBICKI, *Impulsive loading of a spherical container with rigid-viscoplastic and strain rate sensitive material*, Arch. Mech., **15**, 775–790, 1963.

12. A. PABJANEK, *Analysis of viscoplastic cylindrical shells*, IFTR Reports, Polish Academy of Sci., **43**, 1971.

13. T. WIERZBICKI, *An approximate linear theory of viscoplastic shells*, Arch. Mech., **24**, 5-6, 941–953, 1972.

14. W. WOJNO, *Perturbation solution for a rigid-viscoplastic spherical container*, Arch. Mech., **31**, 3, 407–422, 1979.

15. W. WOJNO and T. WIERZBICKI, *Perturbation solution for a rigid-viscoplastic spherical container and for impulsively loaded viscoplastic plates*, Int. J. Appl. Non-Linear Mech., **15**, 211–223, 1980.

16. W. WOJEWÓDZKI, L. KWAŚNIEWSKI and S. JEMIOŁO, *Vibrations of elastic-viscoplastic spherical shell in the range of moderate deflections* [in Polish], Prace Nauk. Polit. Warszawskiej, 114, 6–40, 1992.

17. T. WIERZBICKI and H. ANDRZEJEWSKI, *Impulsive loading of viscoplastic cylindrical shells*, Proc. Symp. Plastic Analysis of Struct., Iassy, 461–479, September 1972.

18. S.R. BODNER and P.S. SYMONDS, *Experiments on the viscoplastic response of circular plates to impulsive loading*, J. Mech. Phys. Solids., **27**, 91–113, 1979.

19. W. IDCZAK, CZ. RYMARZ and A. SPYCHAŁA, *Studies on shock-wave loaded, clamped circular plates*, J. Tech. Phys., **22**, 2, 175–184, 1981.

20. J.W. LEECH, *Finite-difference circulation method for large elastic-plastic dynamically-induced deformations of general thin shells*, Ph. D. Thesis, Dept. of Aeronautics and Astronautics, Massachusetts Institute of Technology, Cambridge, MA 1966.

21. R. SCHMIDT and J.N. REDDY, *A refined small strain moderate rotations theory of elastic anisotropic shell*, ASME J. Appl. Mech., **55**, 611–617, 1988.

22. A.F. PALMERIO, J.N. REDDY and R. SCHMIDT, *On a moderate rotation theory of laminated anisotropic shells. Part I, II*, Int. J. Non-linear Mech., **25**, 687–714, 1990.

23. R. SCHMIDT and D. WEICHERT, *A refined theory of elastic-viscoplastic shells at moderate rotations*, ZAMM, **69**, 1, 11–21, 1989.

24. P. PERZYNA, *Fundamental problems of viscoplasticity*, Adv. in Mech., **9**, 243-377, 1966.

25. J. LEMAITRE and J.-L. CHABOCHE, *Mechanics of solid materials*, Cambridge Univesity Press, Cambridge 1990.

26. S.R. BODNER and Y. PARTOM, *Constitutive equations for elasto-vicoplastic strain-hardening materials*, ASME J. Appl. Mech., **42**, 3, 385–389, 1975.

27. K. WOŹNICA, *Lois de comportement du solide elasto-viscoplastique*, Cahiers de Mécanique, Univ. des Sciences et Techn. de Lille, EUDIL-LML, 2, 1993.

28. A. BEN-CHEICK, *Elasto-viscoplasticité à température variable*, Ph.D. Thesis, Universiteé Paris 6, 1987.

29. T.M. MILLY and D.H. ALLEN, *A comparative study of non-linear rate-dependent mechanical constitutive theories for crystalline solids at elevated temperatures*, Rep. API-E-5-82, Virginia Politechnic Inst. and State University, Blackburg, Virginia 1982.

30. J. ARGYRIS, H. BALMER and I.ST. DOLTSINIS, *On shell models for impact analysis*, The Winter Annual Meeting of the American Society of Mechanical Engineers, Vol. 3, 443–456, Dec. 1989.

31. T. BELYTSCHKO, B.L. WONG and H.Y. CHIANG, *Improvements in low-order shell elements for explicit transient analysis*, The Winter Annual Meeting of the American Society of Mechanical Enginners, Vol. 3, 383–398, Dec. 1989.

32. H.A. BALMER and E.A. WITMER, *Theoretical-exprimental correlation of large dynamic and permanent deformation of impulsively loaded simple structure*, Air Force Flight Dynamics Laboratory, Report FDP-64-108, 1964.

33. A.M. RAJNDRAN, S.J. BLESS and D.S. DAWICKE, *Evaluation of Bodner–Partom model parameters at high strain rates*, ASME, J. Engng. Mat. Tech., **108**, 75–80, 1986.

GDAŃSK UNIVERSITY OF TECHNOLOGY, GDAŃSK
and
UNIVERSITÉ DES SCIENCES ET TECHNOLOGIES DE LILLE,
VILLENEUVE D'ASCQ, FRANCE.

Received October 26, 1994.